Journal of Geodesy (1999) 73: 398–406

Journal of Geodesy

Improvement in global gravity field recovery using GFZ-1 satellite laser tracking data

R. König, Z. Chen, Ch. Reigber, P. Schwintzer

GeoForschungsZentrum Potsdam (GFZ), Div. I, Telegrafenberg, D-14473 Potsdam, Germany
e-mail: psch@gfz-potsdam.de; Tel.: +49 331 288 1131; Fax: +49 331 288 1111

Received: 10 November 1998 / Accepted: 19 April 1999

Abstract. The passive satellite GFZ-1 has been orbiting the Earth since April 1995. The purpose of this mission is to improve the current knowledge of the Earth's gravity field by analysing gravitational orbit perturbations observed at unique low altitudes, below 400 km. GFZ-1 is one target of the international satellite laser ranging ground network. An evaluation of the first 30 months of GFZ-1 laser tracking data led to a new version of the global GRIM4-S4 satellite-only gravity field model: GRIM4-S4G. Information was obtained from GFZ-1 data for spherical harmonic coefficients up to degree 100, which was not possible in any earlier satellite-only gravity field solution. GFZ-1's contribution to a global $5 \times 5°$ geoid and gravity field representations is moderate but visible with a 1 cm and 0.1 mGal gain in accuracy on a level of 75 cm and 5 mGal, respectively.

Key words. GFZ-1 · Global gravity model · Geoid · Precise satellite orbit determination · Gravity satellite missions

1 Introduction

GFZ-1, a passive spherical satellite equipped with laser retro-reflectors, was jettisoned into its orbit from the Russian space station MIR in April 1995. The initial orbit configuration of GFZ-1 therefore was the same as for the MIR station: mean altitude 400 km, inclination 52°, almost zero eccentricity. The mission was initiated, funded and is controlled by GeoForschungsZentrum Potsdam (GFZ). A detailed mission and satellite description is given in König et al. (1996a). The main purpose of GFZ-1 is the improvement of the knowledge of the Earth's gravity field by analysing GFZ-1's orbit perturbations induced by gravitational forces. This implies the careful treatment of air-drag induced orbit accelerations, which are an important error source and quite significant at low altitudes, although these can be used for atmosphere density studies. Meanwhile, as a result of air drag, the altitude of GFZ-1 had decreased by 50 km to about 350 km. With the decay of the orbit, GFZ-1 becomes increasingly more sensitive to irregularities in the Earth's gravity field. Thus, all GFZ-1 tracking data, which are acquired to date and will be acquired until the end of their lifetime, which is expected to come in about 1 year, are of increasing importance for gravity field modelling. A drawback might arise from the hard-to-model surface forces due to air drag, which also increase in amplitude with decreasing altitude.

At the beginning of the mission, GFZ-1 tracking data were evaluated to prove the mission concept and to investigate the capability of GFZ-1 tracking observations for gravity field model improvement, followed by intensive studies of the surface-force parametrization in GFZ-1 precise orbit restitution (König et al. 1997). A first tentative gravity field solution employing GFZ-1 laser data from the first 42 days of the mission was carried out as described in König et al. (1996b). The GFZ-1 normal equation systems were combined with the overall GRIM4-S4 global gravity model normals deduced from optical, microwave and laser tracking data of 34 satellites with a minimum altitude of about 800 km (Schwintzer et al. 1997). It turned out that GFZ-1 data contribute considerably to the solution of gravity coefficients around orders 16, and in an even more pronounced way around orders 31 and 46 in the spherical harmonic expansion of the gravitational potential. These orders are responsible for resonant, i.e. large-amplitude and long-period, perturbations in the orbit. Based upon these first experiences, more complete and more detailed data analyses were performed with the meanwhile-extended data base: optimum GFZ-1 surface force parametrization in precise

Correspondence to: P. Schwintzer

GFZ-1 orbit computation based upon 1 year of GFZ-1 laser data and gravity field modelling from 30 month's worth of data, solving also for spectral terms beyond degree 70, which was the limit in the early solutions.

2 GFZ-1 mission description

GFZ-1 is a spherical satellite with a diameter of 215 mm and a mass of 20.6 kg. Its surface is covered with 60 laser retro-reflectors (Fig. 1). The massive satellite body, made from bronze, features a favourable low area-to-mass ratio. The satellite is designed as a passive laser target like the geodetic satellites LAGEOS, STARLETTE and STELLA (Kramer 1996), but was put into an orbit with the lowest altitude ever flown to date for geodetic purposes. On 19 April 1995, GFZ-1 was released from the Russian space station MIR into a near-circular, medium-inclination (51.6°) orbit with an initial altitude of 400 km. During the expected lifetime of about 5 years, the altitude of the satellite decays at a variable rate depending on the solar and geomagnetic activity (Fig. 2). While decaying, the satellite moves through particular resonance regimes of the gravity field. Figure 3 displays the maximum orbit perturbations per degree and order of the spherical harmonic expansion of the gravity field for the two altitudes 400 and 300 km. Such kind of spectra are discussed in Reigber (1989) and are obtained analytically from the first-order solution of the Lagrange planetary equations (Kaula 1966, Kovalevsky 1989). The deep and shallow resonances become visible and their gradual change with altitude and time. While the altitude decreases, orbit perturbations caused by the gravity field increase. In addition, a slight change in the resonant orders appears due to the fact that resonant order numbers can be found close to multiples of the values of the mean motion of the satellite. During the mission, GFZ-1 will increase its mean motion from approximately 15.5 to nearly 16 revolutions per day. In total, the orbit of GFZ-1 is expected to experience pronounced perturbation caused by the gravitational geopotential, which can be attributed to the harmonic coefficients within the resonant orders around orders 16, 31, 46, 62 and 77 up to degree 100 and more.

At the beginning of the mission, the solar activity cycle was in its low phase. As the altitude of GFZ-1

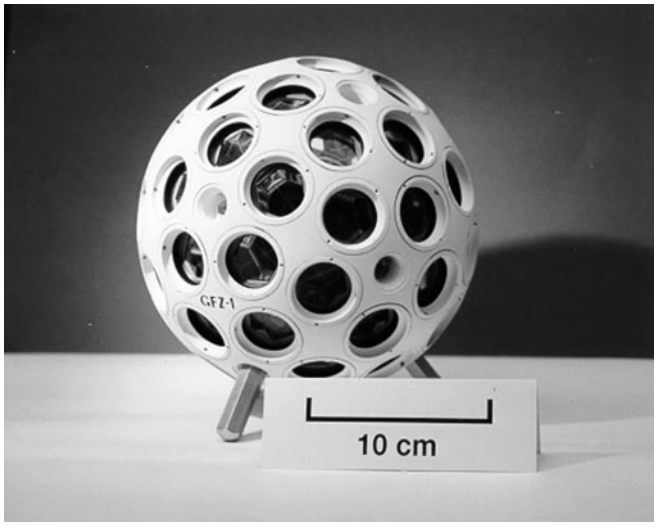

Fig. 1. GFZ-1 satellite

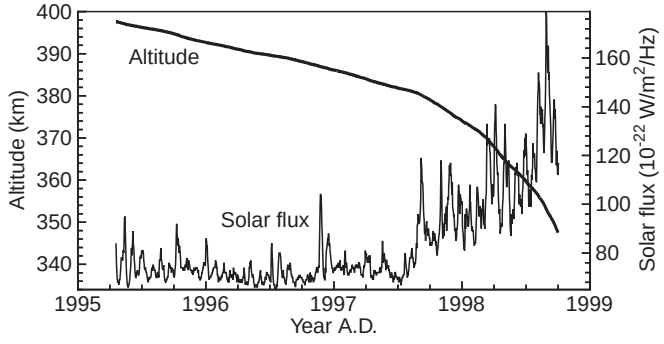

Fig. 2. GFZ-1 orbit decay and solar activity

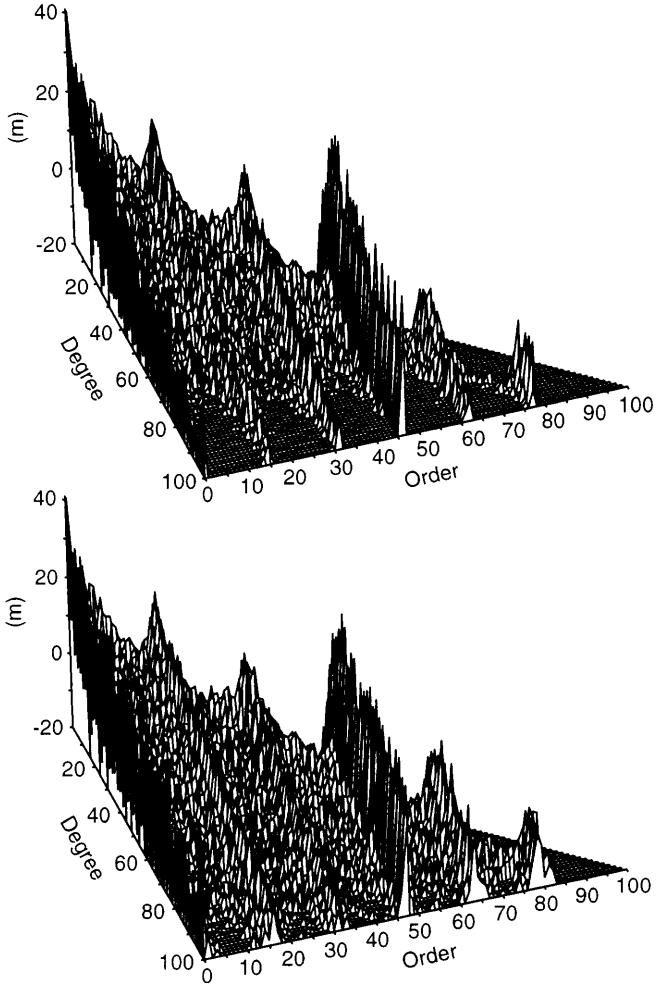

Fig. 3. Maximum GFZ-1 orbit perturbations per degree and order of spherical harmonic gravitational coefficient; altitudes 400 km (*above*) and 300 km (*below*)

decreases with time, solar activity moves towards the maximum of the cycle. Both lower altitude and increased solar activity lead to higher atmospheric density. The orbit perturbations due to atmospheric drag will increase in magnitude and, with time, the mission will become more interesting for the study of atmospheric drag models and more complex with regard to the separation of the gravitational and non-conservative surface force signals in the data.

The exclusive tracking system of GFZ-1 is the weather-dependent satellite laser ranging (SLR) technique. Since the launch of GFZ-1, 33 stations worldwide have participated in GFZ-1 tracking. GFZ-1 is quite a difficult target for SLR tracking. Because of its low orbit, the transit times of only a few minutes over an SLR station are rather short, hardly leaving time for intensive search procedures to acquire the satellite. The fast velocity of the satellite relative to the station and the relatively short laser-pulse travel times between station and satellite imposed challenging requirements on the hardware of most stations at the beginning of the mission. For many stations, tracking of GFZ-1 still is near the limit of, or even beyond, their capabilities. As a result of great efforts and collaborations within the global SLR community, GFZ-1 has been tracked whenever possible. However, the tracking data are not equally distributed in space and time. As shown in Fig. 4, the majority of the data have been acquired in the northern hemisphere, with a high concentration in Europe. Over the southern hemisphere, the only contributions come from two stations in Australia and one station located as the west coast of South America.

The distribution in time of the number of observed GFZ-1 passes (Fig. 5) exhibits periodical minima during daylight tracking conditions over the northern hemisphere. For daylight SLR tracking, extremely high accuracies of orbit predictions are required for targeting in order to distinguish the measurement signal from nuisance signals originating from ordinary sunlight. In GFZ-1's orbit configuration day-/nighttime periods last for about 1 month and switch periodically between the northern and southern hemispheres. Due to the larger

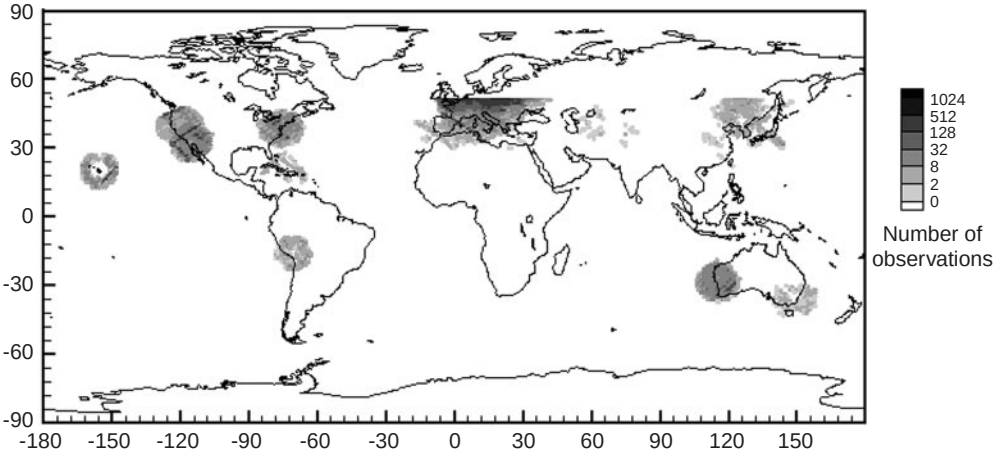

Fig. 4. Geographic distribution of GFZ-1 laser observations (number of observations per $1 \times 1°$ pixel of GFZ-1's ground track)

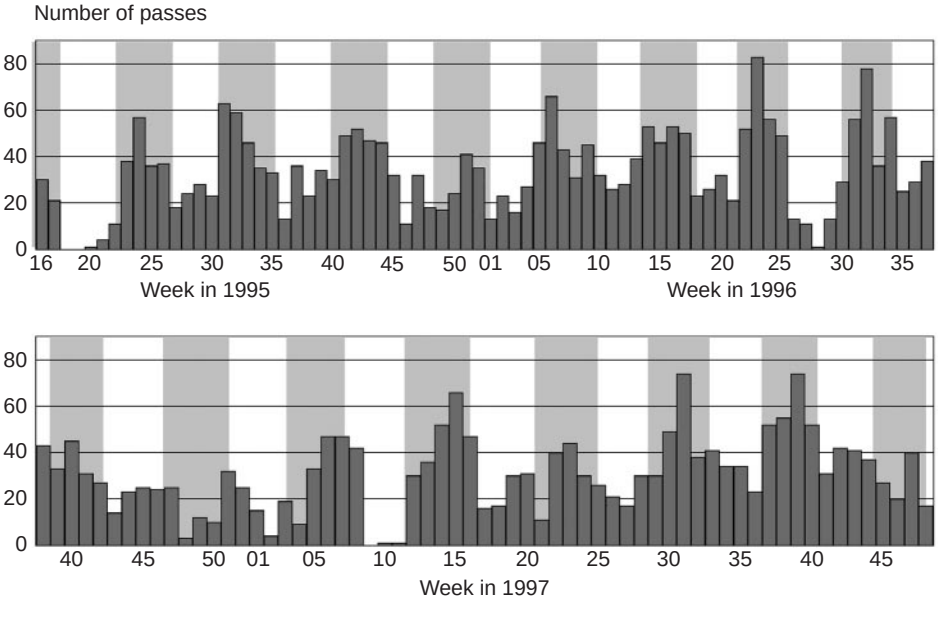

Fig. 5. Number of observed GFZ-1 passes per week and day-/nighttime (bright/grey) tracking conditions in northern hemisphere

number of potential tracking stations in the northern hemisphere, the worldwide amount of acquired data becomes higher during northern nighttime tracking phases.

This unbalanced geometrical configuration prevents a standardized processing in precise orbit and gravity field determination. For these tasks, it becomes necessary to choose carefully the analysis periods with sufficiently dense data coverage, to select deliberatively the parameters for a least-squares (LS) adjustment, and to assess thoroughly the quality of the solutions.

3 Earth gravity field recovery – strategy and results

For all GFZ-1 orbit and gravity field recovery computations, the GRIM4 computational standards, numerical models and procedures, as given in Schwintzer et al. (1997), are applied.

In preparation of the final gravity field solution, the optimum parametrization of the GFZ-1 arcs with respect to non-gravitational surface forces is investigated on the basis of the first half year of GFZ-1 SLR data (April–September 1995). One arc denotes the restitution of GFZ-1's trajectory over a period of, depending on the available amount of data, 4 to 7 days, with one set of initial satellite position and velocity by numerical orbit integration and LS adjustment. Optimum parametrization of surface forces means that both over- and under parametrization have to be avoided in order to prevent absorption of gravitational signal by too many non-gravitational parameters and degradation of the solution by mismodelling, respectively.

For these preparatory investigations, the arc-independent parameters in the arc-wise-generated normal equation systems are the coefficients of a spherical harmonic expansion of the gravitational potential up to degree and order 70, a selected set of ocean tide potential coefficients, and the tracking station position parameters. Six different parametrizations of the arc-dependent surface force parameters are studied, as compiled in Table 1. With each of the six parametrizations, single-arc normal equation systems are generated, accumulated, and combined with the GRIM4-S4 normal equation system into one system which then is solved to yield a

Table 1. Combination of arc-dependent parameters in GFZ-1 orbit computations to absorb mismodelling effects in non-gravitational surface forces

	Combination					
	A	B	C	D	E	F
Scaling factor for solar radiation pressure	y	y	y	n	n	n
Along-track empirical once-per-revolution acceleration	y	y	n	y	y	n
Cross-track empirical once-per-revolution acceleration	y	n	n	y	n	n

y – adjusted, n – not adjusted; 6-hourly scaling factors for atmospheric drag are in all cases adjusted

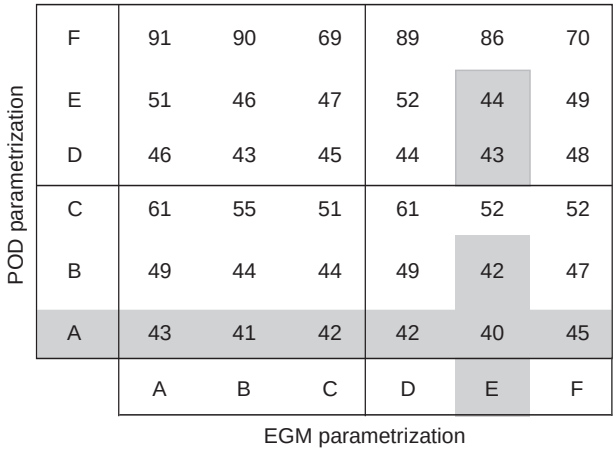

Fig. 6. RMS of orbital fits [cm] in GFZ-1 orbit computations applying different surface force parametrization schemes in Earth gravity model (*EGM*) computations and subsequent test-arc precise orbit determination (*POD*) (see Table 1 for meaning of parameter combinations *A* to *F*)

gravity field model solution from the half year's worth of data. Each of the six gravity field solutions is then employed and tested in precise orbit computations with five GFZ-1 arcs not included in the solution, again adopting different combinations of surface force parameters to be adjusted. The root-mean-square (RMS) values of the orbital fits (RMS of observation residuals in the orbit adjustment) are displayed in Fig. 6. The numbers in a matrix row vary with the parameter combination applied in the GFZ-1 orbit processing for the gravity field solutions, and the variation in a column is due to the chosen parameter combination in the GFZ-1's a posteriori independent test-arc computations.

Obviously, for GFZ-1 arcs the best orbital fits result in gravity field models deduced with parametrization E. The parametrizations C and F result in considerably larger RMS values due to the missing once-per-revolution empirical acceleration terms. These terms are absolutely necessary to absorb shortcomings in the atmospheric density model. On the other hand, all gravitational accelerations coming at the along-track once-per-revolution frequency are then lost for the gravity field model solution. Also, the gravity field models give better orbital fits when the scaling factor for solar radiation pressure is dropped in the gravity field normal equation processing: E better than B, D better than A. Solving for a cross-track empirical once-per-revolution disturbing acceleration is also not favourable for the gravity field model solution: E better than D, B better than A. Parametrization E therefore was eventually adopted for the generation of the gravity field normal equation systems.

From the viewpoint of precise orbit determination, parameter combination A with all parameters switched on of course yields the best orbital fits to the observations. However, the results for the solar radiation scaling factors are far from reality, which points to aliasing with other unresolved dynamic model errors. This is again an argument for not solving for these parameters simultaneously with the geopotential.

Table 2. Location of satellite laser tracking stations contributing to the GRIM4-S4G gravity field model solution

No.	Name	Latitude [deg]	Longitude [deg]	Height [m]
1864	MAIDANAK	38.6	66.9	2719
1868	KOMSOMOLSK	50.6	136.7	265
1870	MENDELEEVO	56.0	37.2	257
1884	RIGA	56.9	24.0	32
1953	SANTIAGO DE CUBA	20.0	−75.7	18
7090	YARRAGADEE	−29.0	115.3	245
7105	GREENBELT	39.0	−76.8	23
7109	QUINCY	39.9	−120.9	1110
7110	MONUMENT PEAK	32.8	−116.4	1843
7210	MAUI	20.7	−156.2	3069
7236	WUHAN	30.5	114.3	39
7237	CHANGCHUN	43.7	125.4	275
7249	BEIJING	39.6	115.8	83
7403	AREQUIPA	−16.4	−71.4	2492
7811	BOROWIEC	52.2	17.0	123
7824	SAN FERNANDO	36.4	−6.2	97
7831	HELWAN	29.8	31.3	130
7835	GRASSE	43.7	6.9	1323
7836	POTSDAM	52.3	13.0	134
7837	SHANGHAI	31.0	121.1	28
7838	SIMOSATO	33.5	135.9	102
7839	GRAZ	47.0	15.4	540
7840	HERSTMONCEUX	50.8	0.3	76
7843	ORRORAL	−35.6	148.9	1350
7918	GREENBELT	39.0	−76.8	22

For the final incorporation of GFZ-1 laser data into the GRIM4-S4 gravity model normal equation system, 95 GFZ-1 arcs were processed with a total of 74 038 observations (mainly 5-s normal points) from 3364 passes observed by the 25 laser ranging stations which are listed in Table 2. The data cover the period April 1995 to November 1997 excluding the month of October 1995, which was left for use in independent test-arc computations to evaluate the gravity model solution later on. After having obtained an optimum orbital fit to the data in an LS orbit adjustment, arc-by-arc normal equation systems were generated, adopting the parameter combination E (Table 1) for the surface force unknowns. Each individual normal equation system then contains the following unknowns:

1. Global unknowns

- Static gravitational potential: spherical harmonic coefficients $\bar{C}_{\ell m}, \bar{S}_{\ell m}$ complete to degree and order $\ell, m = 60$ plus selected terms up to maximum degree 100 for the zonals and around GFZ-1's resonant orders 15/16 and multiples of the first resonant order up to maximum order 93 (5820 unknowns, excluding degree 1 terms and $\bar{C}_{21}, \bar{S}_{21}$ and including C_{00} to scale the initially adopted GM value: the gravitational constant G times mass of Earth M);
- Dynamic gravitational potential: secular rate in $\bar{C}_{20}$ and ocean tide potential coefficients for 8 diurnal and semi-diurnal tides (77 unknowns);
- Geocentric tracking station coordinates (epoch values) plus horizontal rates of change to account for plate-tectonic movements (5 unknowns per station).

The choice of the global unknowns corresponds to the GRIM4-S4 set of unknowns but with an increased number of geopotential unknowns within GFZ-1's (near-)resonant orders.

2. Arc-dependent unknowns

- GFZ-1's position and velocity at initial epoch of each arc;
- Surface forces: 1 to 4 air drag scaling factors per day depending on the actual data distribution along the arc, and amplitude and phase of a periodic along-track acceleration to absorb an unmodelled non-gravitational once-per-revolution disturbance.

The resulting 95 normal equation systems were accumulated, weighted, and finally combined with the 34-satellite normal equation system of the gravity field model GRIM4-S4 (Schwintzer et al. 1997). GRIM4-S4 is complete up to degree/order 60 plus some terms up to maximum degree 69 within the zonals and ERS-1 resonant orders 13 and 57. The GFZ-1 data weighting with a standard deviation of 90 cm was found iteratively relative to the given GRIM4-S4 system to yield an optimum and stable solution. A higher weight on the GFZ-1 data increases the correlations between the solved-for parameters and degrades the solution. The new overall normal equation system including GFZ-1 laser observations was eventually solved simultaneously for the gravitational, tidal and station position parameters, as given above, to yield the GRIM4-S4G satellite-only global gravity field model. Prior to the solution, stochastic a priori information resulting from the pseudo-observation equations

$$\{\bar{C}_{\ell m}, \bar{S}_{\ell m}\} = 0 \pm \sigma_\ell \cdot c^{-1} \tag{1}$$

with $\sigma_\ell = 10^{-5}/\ell^2$ following Kaula's degree variance model (Kaula 1966) and c being an empirical scaling factor, was added to the normal equation system for all harmonic gravitational coefficients with a degree larger than 5. As in the previous GRIM solutions (Schwintzer et al. 1997), the observation equations [Eq. (1)] have to be overweighted by a factor of $c^2 = 100$ when added to the overall normal equation system to be solved by matrix inversion. Due to the attenuation of the gravitational signal with altitude and due to high correlations between the solved-for parameters, a complete solution without any a priori information is not possible. The real spectral resolution of Earth's gravity field models from satellite tracking data available to date is somewhere around degree/order 35, corresponding to a spatial resolution of about 1200 km (full wavelength) at the Earth's surface. This becomes evident when comparing the power spectra per degree of a satellite-only model like GRIM4-S4 and a combination model like GRIM4-C4 incorporating also surface data (Schwintzer et al. 1997). Due to the attenuation of the gravity signal with altitude, the power rapidly decreases at higher degrees for any satellite-only solution (Lemoine et al. 1998). Higher-degree information is only recoverable from satellite orbit perturbations in bands

around specific orders of the spectral representation of the gravitational geopotential.

The rationale behind restricting this study to a satellite-only gravity field solution, i.e. not including surface gravity and altimeter sea-surface observations, is to obtain better insight into the contribution of GFZ-1 data, especially within the spectral domain of the gravitational potential, and the need of satellite-only geoid models for the recovery of the sea surface topography from altimeter data (Wunsch 1993). To date, the geoid derived from a satellite-only solution can be employed as a reference surface for the sea-surface topography with its 1-m signal only up to about degree/order 13 (λ = 3000 km). At this truncation level the geoid's commissioning error is less than 10 cm, thus giving a reasonable signal-to-noise ratio. In the combined solution EGM96 (Lemoine et al. 1998), the sea-surface topography was solved simultaneously with the geopotential parameters complete to degree/order 20 representing the state of the sea-surface topography at the time periods covered by the altimeter data in the solution.

4 gravity field model evaluation – impact of GFZ-1 SLR data

By an a posteriori partial redundancy decomposition using the pseudo-observation equations [Eq. (1)], one can compute for each individual solved-for gravitational coefficient the information content coming from the tracking data relative to that artificially introduced via the stochastic a priori information (Schwintzer 1990). The more the a priori information dominates, the more the coefficient is constrained to zero. Figure 7 depicts the resolution indices f_i for the adjusted gravitational coefficients per degree and order of the GRIM4-S4G solution which are equivalent to the partial redundancies of the pseudo-observations introduced in Eq. (1)

$$f_i = 1 - q_{ii} \cdot c^2/\sigma_\ell^2 \tag{2}$$

with q_{ii} being the diagonal term of the a posteriori co-factor matrix of the gravitational unknowns $x_i = \{\bar{C}_{\ell m}, \bar{S}_{\ell m}\}$. The indices f_i range from 0 (i.e. the coefficient is not at all sensed by the tracking data) to 1 (i.e. the coefficient is fully recoverable from the total of orbit observations). Figure 7 reveals the typical pattern for a satellite-only solution: complete coverage of the very long wavelength part of the gravitational spectrum and a higher resolution only for certain bands of orders which are associated with resonant and near-resonant orbit perturbations of low Earth-orbiting satellites.

Figure 8 shows the difference in resolution between the GRIM4-S4G solution and the basis model without the GFZ-1 data. An increase in resolution through the incorporation of the 30 month's worth of GFZ-1 data can be recognized in particular for the terms around GFZ-1's resonant orders 16, 31, 46, 62 and 77 (up to degree 100), which corresponds to the analytical orbit perturbation spectrum (Fig. 3). GFZ-1's contribution is especially pronounced between the 2nd (order 31) and 3rd (order 46) resonant order for tesseral terms from degree 40 to 60, which until now have hardly been sensed by any other satellite. Figure 8 can also be derived from the differences in the diagonal terms of the co-factor matrices of both parameter solutions because the partial redundancies are derived from these terms. Therewith this figure also indicates the relative gain in precision when adding GFZ-1 data to the gravity field solution.

Figure 9 shows the square roots of signal variances per degree of the spherical harmonic expansion of the geopotential in terms of geoid heights for both models GRIM4-S4G and GRIM4-S4, including and excluding GFZ-1 data, respectively. For comparison, the corresponding curve derived from Kaula's degree-variance model, scaled down by a factor of $\sqrt{0.5}$ (Lerch et al. 1979) to be closer to reality, is also given in Fig. 9. Kaula's (corrected) curve represents a smoothed spectrum of the full geoid's power per degree. The lack of

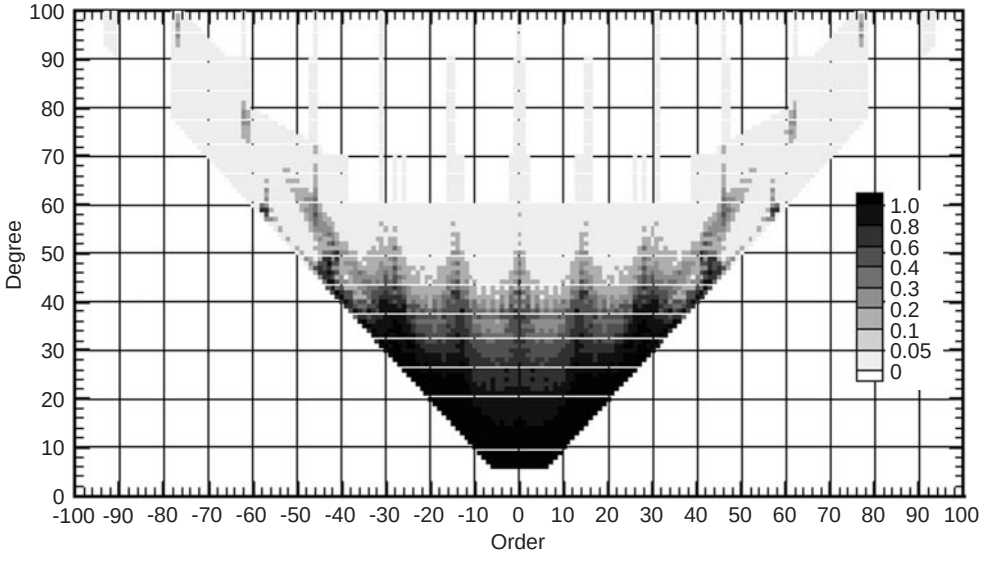

Fig. 7. Resolution indices (partial redundancies of stochastic a priori information equations) of the GRIM4-S4G gravity field solution per degree and order of coefficients (*1* fully resolved, *0* not sensed at all)

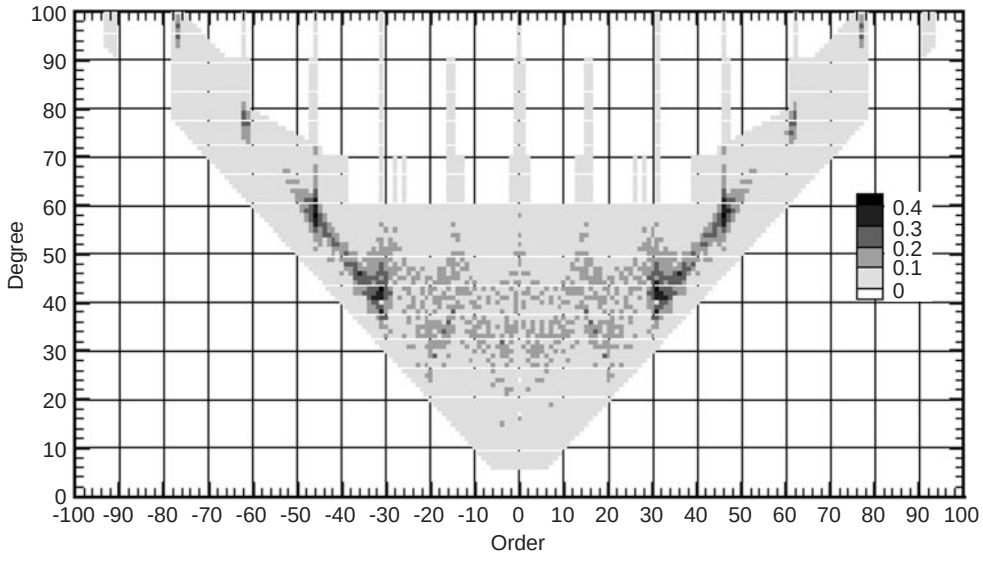

Fig. 8. Increase in resolution indices per degree and order of coefficients by incorporating GFZ-1 data in the gravity model solution (GRIM4-S4G vs GRIM4-S4)

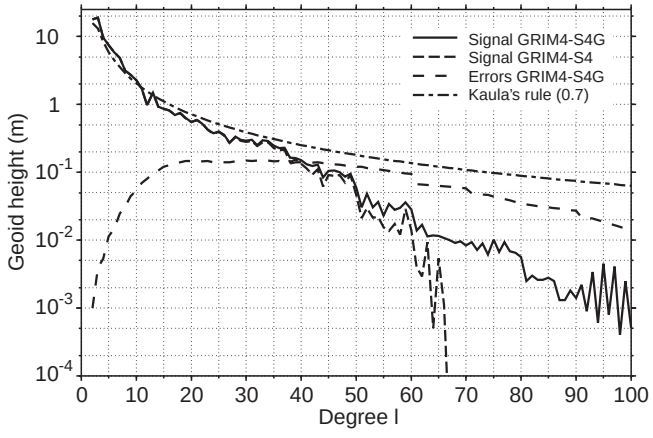

Fig. 9. Square root of signal and error variances per degree of the gravitational model's spectrum in terms of geoid heights

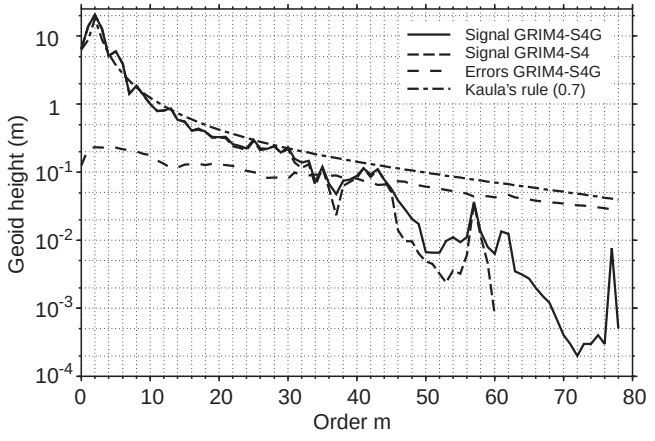

Fig. 10. Square root of signal and error variances per order of the gravitational model's spectrum in terms of geoid heights

power of both GRIM4 curves beyond degree 35 is due to the attenuation of the gravitational signal with the satellite's altitude. Also, the signal-to-noise ratio for the accumulated signal per degree, rapidly decreases with increasing degree, as can be deduced from Fig. 9, where also the estimated error spectrum is plotted. The effect of adding 30 months' worth of GFZ-1 data can clearly be recognized by an increase in power from degree 30 onwards for the GRIM4-S4G model. The gain in power is especially pronounced between degrees 50 and 60, although the cummulative signal per degree still is far below its estimated error. The commission error in the geoid deduced from all the adjusted coefficients up to maximum degree 100 accumulates to roughly 1 m, not taking into account the truncation error due to the lack of full resolution.

Figure 10 shows the geoid signal and error spectra of the same models as in Fig. 9, but per order of the spherical harmonic expansion. As a satellite basically 'sees' the gravity field per order (cf. Fig. 3), this kind of presentation may be more illustrative. It is demonstrated that GFZ-1 data mainly add power to those orders which until now have been less well resolved in a satellite-only model: orders 37 and 46 through 56.

The geographical distribution of the differences between the geoids derived from the GRIM4-S4G and GRIM4-S4 spherical harmonic models is shown in Figure 11. In terms of $1 \times 1°$ block mean values, the differences range from -1.5 to 1.7 m with an RMS of about 25 cm.

The regular wave pattern, which can be detected in the geoid differences, follows GFZ-1's ground track near the 32 rev/2 days resonant orbit. From perturbations at this orbit frequency, the largest changes in the recovered gravity field model are induced. In view of the 70-cm overall commissioning error in a $5 \times 5°$ geoid representation of a present-day satellite-only gravity field model, the identified geoid differences between a solution with and without GFZ-1 data are not significant and lead to only a 1-cm improvement (from 75 to 74 cm) in the RMS of differences when compared with a homogeneous $5 \times 5°$ ocean geoid derived from altimetry. The corresponding improvement in terms of gravity anomalies amounts to 0.1 mGal on a level of 5 mGal.

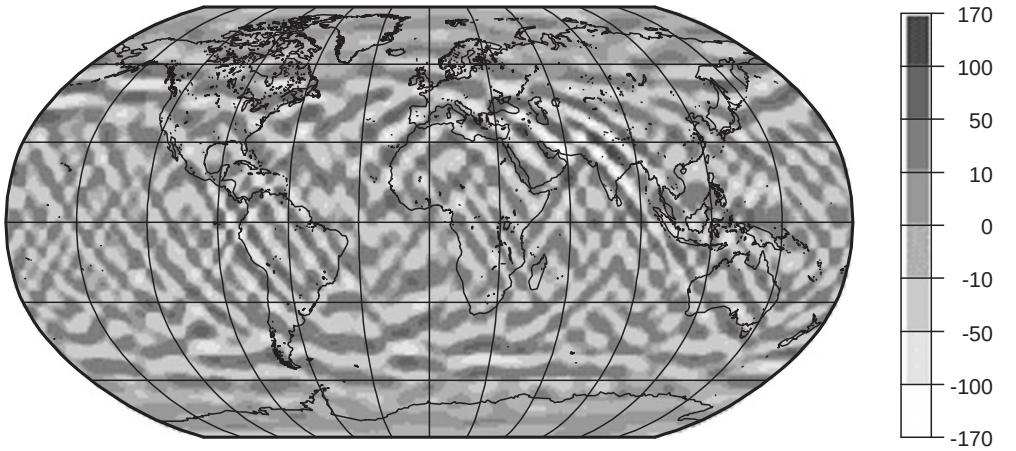

Fig. 11. Difference in $1 \times 1°$ geoid heights [cm] deduced from the GRIM4-S4G and GRIM4-S4 gravity models

Table 3. GFZ-1 test-arc computations for different degrees of truncation and gravity field models

Max. degree	60	70	80	100
GRIM4-S4	248	–	–	–
GRIM4-S4G	43	33	28	28
EGM96	57	37	32	42

Values give RMS (cm) of orbital fits over five independent 6d arcs

Using GFZ-1 tracking data from October 1995, which intentionally is not included in the GRIM4-S5G solution, five test arcs were composed to evaluate the performance of the solution in GFZ-1 precise orbit computation. Table 3 gives the RMS of the orbital fit to the laser ranges after the orbit adjustment when applying parameter set E (see Table 1). The RMS values are given for different truncation degrees. The results clearly demonstrate that the GFZ-1-sensitive terms are insufficiently modelled in the GRIM4-S4 solution lacking GFZ-1 data, and emphasize the importance of solving for higher degree/order terms which between degrees 71 and 80 account for another 5 cm of improvement in GFZ-1's orbital fits. The sensitivity of GFZ-1's orbit to these high-degree terms is also visible in the orbit restitution results from applying the EGM96 gravity field model (Lemoine et al. 1998), where the orbital fit is degraded when taking into account terms between degrees 81 and 100. EGM96 includes some 5000 GFZ-1 laser ranges. The basic satellite-tracking-data normal equation system in the combination solution EGM96, however, was complete to only degree 70. For higher-degree terms, information comes from surface gravity and altimeter data.

The performance of GRIM4-S4G in higher-altitude satellites' orbit determination, compared to GRIM4-S4, is slightly better for e.g. STARLETTE (9.7 vs 9.9 cm), whereas for other satellites like ERS-1, Ajisai (Kramer 1996) and the very high LAGEOS satellites no change in the precision of orbit restitution can be realized. The test-arc results support the conclusion that the GFZ-1 data were properly modelled and processed without inducing systematic errors in the gravity field solution which would show up in a degraded performance in precise satellite orbit determination.

5 Conclusions

The exploitation of 30 months' GFZ-1 laser data with altogether about 74 000 data points has resulted in the new satellite-only gravity field model GRIM4-S4G based upon an earlier GRIM4-S4 solution deduced from 2.8 million tracking observations obtained on 34 other satellites. The model GRIM4-S4G in its spherical harmonic spectral representation is complete to degree/order 60 with higher-degree terms solved for the zonals and resonant bands around orders 15/16 and higher resonances up to the 6th resonance at order 93, where terms up to maximum degree 100 were resolved.

In spite of the relatively small number of observations, the gain in information, especially around the resonant orders, is quite remarkable. The significance of higher-degree terms up to degree 80 is proved in GFZ-1 precise orbit computations. The GFZ-1 contribution to a global $5 \times 5°$ geoid and gravity field representation is moderate but visible, with a 1 cm and 0.1 mGal consistent gain in accuracy on a level of 75 cm and 5 mGal, respectively. These figures will slightly improve if GFZ-1 is observed over the remainder of its lifetime. Due to the decaying orbit, the gravitational orbit perturbation spectrum varies and resonances then gradually shift by one order. Due to the system-inherent sparse laser tracking, no overall improvement in the recovery of the very-long-wavelength spatial features of the geoid, important for oceanographic applications, can be recognized.

The insufficient coverage of GFZ-1's orbit with tracking data does not allow the exploitation of the full spectrum of gravity-induced orbit perturbations. A breakthrough in gravity field recovery can therefore only be expected from the coming dedicated gravity missions such as CHAMP (Reigber et al. 1999, unpublished) and GRACE (Davis et al. 1996) with active satellites using continuous high–low GPS and low–low ultra-precise microwave satellite-to-satellite tracking, respectively. Highest resolutions can be obtained by applying space

gradiometry, i.e. measuring on board in-situ gravity gradients as foreseen for ESA's GOCE mission (Schuyer 1997).

The spherical harmonic coefficients of the GRIM4-S4G global gravity model are available via file transfer protocol (ftp) upon request to R. König or P. Schwintzer (e-mails: rolf.koenig@dlr.de; psch@gfz-potsdam.de).

References

Davis ES, Melbourne WG, Reigber Ch, Tapley BD, Watkins MM (1996) GRACE – an SST mission for gravity mapping. Suppl to EOS Trans American Geophysical Union (AGU) 77: 40

Kaula WM (1966) Theory of satellite geodesy. Blaisdell, Waltham, MA

König R, Bode A, Chen Z, Grunwaldt L, Neubert R, Reigber Ch, Schwintzer P (1996a) The GFZ-1 mission: design, operations and first results. GFZ Scientific Technical Report STR96/09. GeoForschungs Zentrum, Potsdam

König R, Schwintzer P, Bode A, Reigber Ch (1996b) GFZ-1: a small laser satellite mission for gravity field model improvement. Geophys Res Lett 23: 3143–3146

König R, Bode A, Chen Z, Reigber Ch (1997) Surface forces parametrization of GFZ-1 orbits and gravity field recovery. Adv Space Res 19: 1677–1680

Kovalevsky J (1989) Lectures in celestial mechanics. In: Sansò F, Rummel R (eds) Theory of satellite geodesy and gravity field determination. Lecture notes in Earth sciences, vol 25. Springer, Berlin Heidelberg New York, pp 69–114

Kramer HJ (1996) Observation of the Earth and its environment, survey of missions and sensors. Springer, Berlin Heidelberg New York

Lemoine FG, Pavlis NK, Kenyon SC, Rapp RH, Pavlis EC, Chao BF (1998) New high-resolution model developed for Earth's gravitational field. EOS Trans American Geophysical Union (AGU) 79: 113–118

Lerch FH, Klosko SM, Laubscher RE, Wagner CA (1979) Gravity model improvement using GEOS3 (GEM9 and 10). J Geophys Res 84: 3897–3915

Reigber Ch (1989) Gravity field recovery from satellite tracking data. In: Sansò F, Rummel R (eds) Theory of satellite geodesy and gravity field determination. Lecture notes in Earth sciences, vol 25. Springer, Berlin Heidelberg New York, pp 197–234

Schuyer M (1997) European Capabilities and Prospects for a Spaceborne Gravimetric Mission. In: Sansò F, Rummel R (eds) Geodetic boundary value problems in view of the one centimeter geoid. Lecture notes in Earth sciences, vol 65. Springer, Berlin Heidelberg New York, pp 569–589

Schwintzer P (1990) Sensitivity analysis in least squares gravity field modelling by means of redundancy decomposition of stochastic a priori information. Rep PS/51/90, Deutsches Geodätisches Forschungs institute (DGFI), Dept I, München

Schwintzer P, Reigber Ch, Bode A, Kang Z, Zhu SY, Massmann FH, Raimondo JC, Biancale R, Balmino G, Lemoine JM, Moynot B, Marty JC, Barlier F, Boudon Y (1997) Long-wavelength global gravity field models: GRIM4-S4, GRIM4-C4. J Geod 71: 189–208

Wunsch C (1993) Physics of ocean circulation. In: Rummel R, Sansò F (eds) Satellite altimetry in geodesy and oceanography. Lecture notes on Earth sciences, vol 50. Springer, Berlin Heidelberg New York, pp 9–98